JOURNAL OF Materials CHEMISTRY

Photophysical characterization of dilute solutions and ordered thin films of alkyl-substituted polyfluorenes

Julie Teetsov and Marye Anne Fox*†

Department of Chemistry, University of Texas at Austin, Austin, TX 78712, USA

Received 9th April 1999, Accepted 23rd June 1999

Absorbance and fluorescence spectra of dilute solutions and thin films of polyfluorene rigid-rod polymers **1–3** bearing two hexyl, octyl, or dodecyl groups at the 9-position define the effect of polymer chain interactions on excited state relaxation. Film morphology is controlled by annealing of 250 nm thick films. Under these conditions, the degree of interchain interaction follows the degree of thermotropic liquid crystalline ordering which is, in turn, a function of the length of the attached alkyl substituents. Alkyl substituents also affect the solubility of these polymeric liquid crystals in organic solvents; low solubility favors strong ground state aggregation, as is evidenced by a red-shifted absorption band. In the annealed films, aggregate and excimer formation is evidenced by a broadening of the absorbance band, an increase in the intensity of the low energy emission, the appearance of new long-lived fluorescent species, and structure-dependent changes in observed fluorescence quantum yields.

1. Introduction

There is great interest in the fundamental optoelectronic properties of rod-like conjugated polymers because of their utility in light-emitting devices,[1] lasers,[2] thin film transistors,[3] and polarizers.[4] Polyfluorenes,[5–13] poly(phenyleneethynylenes),[4,12,14] poly(*p*-phenylenes),[15] and derivatives of polyphenylene[16,17] and poly(*p*-phenylenevinylenes)[18] fit into a class of rigid-rod blue light-emitting polymers.[19] The extended conjugation that is characteristic of these families enhances charge delocalization by virtue of the greater molecular planarity attained along their rigid backbones. This electronic delocalization also influences a number of the polymers' physical properties including their band gaps, absorption coefficients, and emission quantum yields.[2]

Rigid–rod polymers often also form stable liquid crystalline phases and self-organize in the solid state either upon heating (thermotropic) or upon adding solvent (lyotropic). Studies of the absorption and fluorescence[4,14,20–22] of several rigid-rod polymers show that appended alkyl side chains can affect both liquid crystallinity and interpolymer interactions. Little is known, however, about the correlation between the shifts in molecular packing and trends in the efficiency of light emission. In fact, one important reason for studying a family of closely related polymers differing only in the length of the attached alkyl chains is to examine whether rigid-rod polymers aligned over large areas can display high degrees of dichroic absorption and emission. With optimal mechanical alignment, interpolymer interactions may serve to enhance the observed dichroic ratio because of the enhanced on-axis dipole moment of the aggregate array compared with that of the individual molecule or a randomly dispersed film. For example, Grell *et al.*[11] have shown an increase in the dichroic ratios from 7 to 20 upon inducing aggregation in their polymer films.

It is also known that interchain π,π* interactions can influence the net observable fluorescence efficiencies in this series through both ground state aggregation and excimer formation. Ground state aggregates formed between two or more polymer chains are evidenced by a broadening of the absorption spectra[23] or by the appearance of new absorption bands.[8] Excimer formation, *i.e.*, complexation between an excited state of a molecule and the same species in the ground state, is particularly favorable in rigid-rod polymers[24] because molecules with extended π-systems are known to adopt even more planar geometries in the excited state, thus facilitating aggregation through π-stacking.[11] Because both ground state aggregates[23,25] and excimers[21,26] can enhance non-radiative decay in solution and in the solid state, aggregation is often considered undesirable in light-emitting devices. Nonetheless, recent work by Grell *et al.*[11] with poly(dioctylfluorene) suggests that fluorescence efficiency may, in fact, increase in the solid state compared with that observed in homogeneous solution.

According to Bradley *et al.*,[8] polyfluorenes form clusters in solvents with poor solvating characteristics and in thin films prepared either from poor solvents or by spin-coating from good solvents while the support is cooled to −77 °C and warmed slowly to induce thermodynamically controlled aggregation. However, the effect of aggregation on observable fluorescence lifetimes and quantum yields is still unclear because evidence for a correlation of either excimer or aggregate formation with the observed fluorescence efficiency is very sample-dependent.[27]

Because the correlation between local order and emission efficiency remains ambiguous, we sought to study interchain interactions of liquid crystalline 9,9-dialkylpolyfluorenes **1–3** with polymer lengths that significantly exceed the effective π-conjugation length. We are particularly

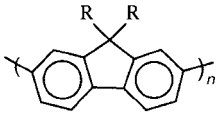

1) R = *n*-C_6H_{13}; **2**) R = *n*-C_8H_{17}; **3**) R = *n*-$C_{12}H_{25}$; *n*=40-65.

interested in observing the influence of the alkyl chain length on spectral trends and excited state lifetimes within the series, hoping that we may discern design features that will assist in preparation of new high efficiency LEDs. In this study, we describe aggregate and excimer formation in a series of dialkylated polyfluorenes **1–3** in solution and as thin films. By determining trends in fluorescence lifetimes and fluorescence quantum yields, we establish that the length of the linear alkyl side chain does indeed play an important role in controlling interchain interactions. In addition, we show that the rigidity of these polymeric liquid crystals, as related to their effective conjugation length, is influenced by the alkyl substituents and that it is therefore possible to control attainable local order in pristine and annealed liquid crystalline thin films by synthetically modifying the length of the attached chain.

† *Present address*: Office of the Chancellor, Box 7001/Holladay Hall, North Carolina State University, Raleigh, NC 27695–7001, USA.

2. Experimental

2.1. Instrumentation

Fourier-transform infrared spectra were obtained as KBr pellets on a Nicolet 510P spectrometer. Gel permeation chromatography (GPC) on Waters Styragel columns with THF as eluent gave peaks that were calibrated against commercial polystyrene standards. (Although GPC calibration against polystyrene standards is a routine procedure for estimating molecular weights of rigid-rod polymers, some recent work has shown these values to be roughly a factor of 3 larger than those attained by light scattering.[11] Here, however, the estimated molecular weights agree roughly with those expected from the additive extinction coefficients of the appended fluorenyl groups.)

Liquid crystalline phase transitions were determined with a Perkin Elmer Series 7 UNIX differential scanning calorimeter (DSC). Thermal decomposition was determined with a Perkin Elmer Series 7 Thermal Gravimetric Analyzer (TGA). Crystalline transitions for bulk and thin films were identified with an Olympus polarizing light microscope (PLM) equipped with a camera attachment and hot and cold stages.

2.2. Materials

Samples **1–3** were a gift from Drs Edward Woo and Michael Inbasekaran from Central & New Businesses R & D, Dow Chemical Company, Midland, Michigan. All other materials (Aldrich) were used as received.

2.3. Thin film preparation

Thin films were prepared with a Specialty Coating Systems Inc. Spin Coater, model P6204-A. Polymer solutions (3 wt.%) prepared in toluene were placed on 1 cm glass squares. The substrate was rotated at a 500 rpm ramping speed for 1 s, followed by 3000 rpm for 30 s, producing 250 ± 30 nm thick films, as determined by a Tencor Instruments Alpha Step 100 profilometer. Films were used as spun or were annealed under Ar at either 160 or 250 °C for 2 h before being cooled at 30 °C min^{-1} to preserve the order of the polymer's liquid crystalline phase. Near-field optical microscopy results show order at 200 nm in pristine films of **3** to a greater extent than in **2**, with essentially complete disorder observed with **1**. After annealing, films of **1** show the greatest order, followed by those of **2** and **3**.

2.4. Transient and steady-state spectroscopy

Absorbance spectra were recorded on a Shimadzu spectrometer. Fluorescence measurements were made with an SLM Aminco SPF 500 fluorimeter. Temperature-dependent measurements were performed with a water-blanketed quartz cuvette. Time-resolved fluorescence lifetimes were obtained at the Center for Fast Kinetics Research by time-correlated single-photon counting using a mode-locked, synchronously pumped, cavity-dumped dye laser ($\lambda = 300$ and 340 nm, 3 μJ $pulse^{-1}$).[28] Emissive photons were collected at 90° with respect to the excitation beam (300 nm) and were passed through a monochromator to a Hamamatsu Model R2809U micro-channel plate. Data analysis was conducted after deconvolution of the instrument response function (fwhm ~80 ps). All solutions were purged with N_2 for 5 min before the measurement and had an optical density (OD) = 0.1 at 340 nm.

2.5. Fluorescence quantum yields

Solution quantum yields were measured relative to 9,10-diphenylanthracene ($\Phi = 0.9$ in cyclohexane)[29] using an SLM Aminco SPF 500 fluorimeter. A Lab Sphere 10 cm integrating sphere was used to obtain absolute quantum yields following the method of de Mello *et al.*[30] Laser excitation (10 mW 355 nm laser pulses) and sample emission were focused into and out of the integrating sphere using fiber optics. All spectra were corrected for the monochromator and photomultiplier tube (PMT) spectral response. Incident radiant energy was converted to a specified number of photons by multiplying the observed emission intensity by wavelength. The observed emission intensity was obtained by integrating over all emission wavelengths in the additive spectrum, where each wavelength's intensity was obtained from an average of 50 decays. Laser drift introduced an approx. 6% relative standard deviation (measured over the duration of each sample measurement). Each reported quantum yield is an average of 2–3 sample measurements with an estimated 10% relative standard deviation.

3. Results and discussion

3.1. Polymer properties

As established by polarizing light microscopy, polymers **1–3** exist as polycrystalline yellow flakes whose molecular weights were characterized by GPC (Table 1), displaying regions of order with dimensions exceeding one micron. Polymers **1–3** readily dissolved (100 μg mL^{-1}) in toluene, chloroform, and THF to yield clear violet solutions. The polymers could be dissolved in dichloromethane, cyclohexane, and *n*-heptane only upon heating. The resulting clear violet solution quickly turned translucent yellow upon cooling, with the formation of a gel or precipitation of the polymer. The yellow color is assigned to a polymer aggregate[8] which shows a new absorption band at 437 nm (see below). The appearance of the 437 nm band in poor solvents results from a mismatch of Hildebrandt parameters.[11] In contrast to polymers **1** and **3**, at room constant temperature and a 10 μg mL^{-1} concentration, polymer **2** began to form aggregates in toluene and tetrahydrofuran, as evidenced by the appearance of the characteristic 437 nm peak. These two latter solvents have better matched Hildebrandt parameters.

Bulk thermal properties of **1–3** were determined with both DSC and PLM (Table 2). These techniques complement each other because DSC is the more sensitive thermal technique, but does not allow for visual observation of bulk polymer or thin film morphology. In pristine films not previously subjected to heating cycles, an endothermic crystalline-to-nematic A liquid crystalline phase transition followed by a second endo-

Table 1 Molecular weights of the poly(dialkylfluorene)s

Polymer	M_n[a] ± 500	PD[b] ± 1	n[c] ± 2
1	17 000	4.1	51
2	24 000	4.4	62
3	21 000	2.6	42

[a]Number averaged molecular weights (M_n). [b]Polydispersities (PD) are determined by GPC *vs.* polystyrene standards in THF, where PD = M_n/M_w (number averaged/weight averaged molecular weight). [c]The number of monomer repeat units (n) is calculated from the M_n.

Table 2 Thermal properties of the poly(dialkylfluorene)s[a]

	Temp./±2 °C (ΔH/±0.01 J g^{-1})			
Polymer	SP	N(A)	N(B)	I
1	94	162–213 (3.69)	222–246 (3.67)	290–300
2	72	80–103 (11.63)	108–157 (11.05)	278–283
3	47	62–77 (0.58)	83–116 (4.57)	116–118

[a]Determined by differential scanning calorimetery and polarized light microscopy of pristine polymers without thermal pretreatment. SP and I refer to softening and melting (isotropic) point. N(A) and N(B) refer to nematic A and nematic B liquid crystalline phases.

thermic nematic A to nematic B liquid crystalline transition is observed in **1–3**, Table 2. These phases are quasi-reversible, with the distribution among phases depending on cooling rates.

The materials can be recycled among these phases without evidence of degradation.[7] Films of **1–3** annealed to a temperature just above the second nematic liquid crystalline transition and then cooled rapidly to preserve liquid crystalline order produce arrays with enhanced crystalline areas, consistent with the observations of Grell *et al.*[7] The softening and melting of polymers **1–3** are not clearly observed by DSC, but softening and melting ranges are reported from PLM hot stage observation. Long alkyl chains have been shown to decrease the liquid crystalline phase transition temperature in rigid–rod polymers by increasing entropy by accessing a larger number of contributing conformations.[31] Consistent with this generalization, our DSC data (Table 2) show that the temperature of the liquid crystalline phase transition is lowest for **3**, followed by **2** and **1**.

PLM was also used to characterize thin films (250 nm thick) at room temperature. The films of **1–3** are considered amorphous because of the absence of birefringence under crossed polarizers in their pristine states (before annealing). In contrast, annealed films displayed high birefringence under these conditions because of the order of their thermotropic liquid crystalline states. The liquid crystalline states of **1–3** are characterized as nematic because of the characteristic Schlieren texture[32] observed by PLM (Fig. 1). This texture results from lamella (made of polymer chains) which form around nucleation points at defects on the surface of the glass substrate.[33,34]

Polyfluorene thin films have excellent chemical stability in the presence of oxygen, moisture, and light as evidenced by the absence of new spectral bands in the IR. For example, there is no evidence for the presence of carbonyl absorbances which might have been introduced by possible photooxidation.[13] Bliznyuk *et al.* have observed, for example, that end-capped polyfluorenes form fluorenones, by a process which is impossible here by virtue of the bisalkylation at the 9-position. In addition, transient emission spectra exhibit unchanged kinetic profiles in both pristine and annealed films, even after more than one week of exposure to ambient laboratory conditions. Nor did thermal gravimetric analysis (TGA) show any change in mass until above 400 °C for **1–3**.

The polymer films **1–3**, however, do show a new absorption band at 437 nm upon heating which is not present in dilute solution or in a pristine film. When a film of **2** that was spin cast from toluene and heated to 250 °C to induce the 437 nm peak was redissolved in toluene, its solution spectra did not display the 437 nm peak. Nor did the redissolved polymer show any change in molecular weight by GPC. Thus, the heating cycle takes place without permanent (covalent) crosslinking or decomposition. Similarly, a bulk sample of **2** was heated to 250 °C, dissolved in toluene, and spun to produce a typical film. The absence of the 437 nm peak under these conditions shows that this peak is due to aggregation, rather than to decomposition of the film. Polymer films were thus assumed to be stable within the heating range (25–250 °C) of our experiments.

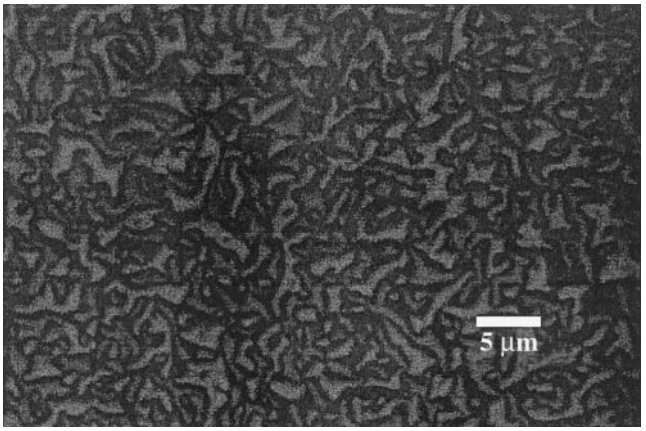

Fig. 1 Polarized light micrograph (magnified 800×) showing characteristic nematic liquid crystalline Schlieren texture of a 250 nm film of **1** annealed at 250 °C (scale bar equals 5 μm).

3.2. Spectral characterization

Solution phase absorbance spectra of **1–3** are similar in bandwidth, absorption maximum, and intensity in toluene and THF. Absorbance spectra of **1–3** at concentrations greater than 10 μg mL^{-1} or in poor solvents such as *n*-heptane or cyclohexane show the same band at 437 nm as was observed in the heated films, Fig. 2. Because this peak is reversible and dependent on concentration, temperature, and solvent, it is also most likely a result of polymer aggregation.[8,11] The degree of aggregation (as established by the intensity of the 437 nm band) is greatest in **2**, followed by **1** and **3**. This suggests that the octyl chain length may provide the optimal supramolecular ordering in this series of polyfluorenes in solution.

Absorbance spectra of pristine films of **1–3** are also similar in λ_{max} and intensity (Fig. 2B), with absorption maxima similar to those observed in solution, Fig. 2A. These films lack evidence of the 437 nm aggregate band, although the bandwidth is broadened from that observed in solution. Annealing of the films causes further broadening, Fig. 2C, and induces the appearance of the absorption at 437 nm. A similar low energy absorption band has been described in the aggregate produced in films of ladder-type poly(*p*-phenylene)[23] and poly(phenyleneethylene),[14] as well as in poly(dioctylfluorene) films cooled to −78 °C and slowly heated to ambient temperatures to induce aggregation.[11] Spectral broadening was attributed to a broader distribution of effective conjugation lengths consequent to polymer π,π* interactions in the ground state aggregates.[23]

Fluorescence spectra of **1–3** in solution are also similar in bandwidth, the wavelength of emission, and intensity (Table 3), implying that the lengths of the appended alkyl chains do not appreciably change the excited state surface of the polymer in solution. Emission from pristine films of **1–3** is red-shifted from their solution phase fluorescence maxima, with the greatest shift being observed in **3**. Annealing further red-shifts the emission of films of **2** and **3**, but not of **1.** Fig. 3

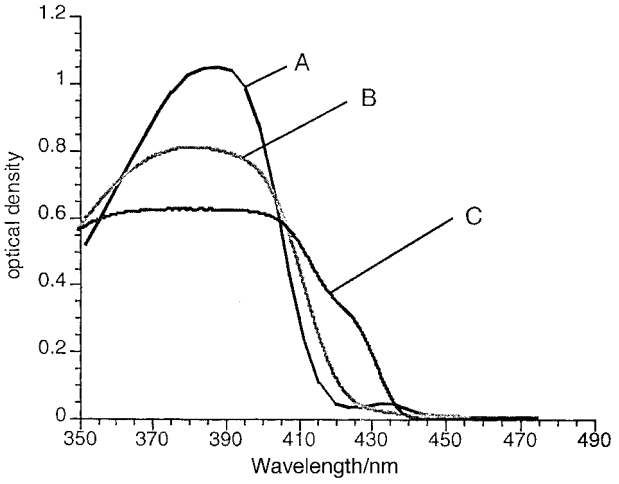

Fig. 2 Absorbance spectra of **2**: A) as a 10^{-4} M solution in THF; B) as a 250 nm pristine (amorphous) film; C) film (B) annealed to 160 °C. A is normalized to B and C at 440 nm for ease of comparison of intensity of the long wavelength aggregate band.

Table 3 Red-shifted emission of poly(dialkylfluorene) films

Polymer	Solution[a] λ_{max}/nm of 2nd vibronic peak	Pristine film[b] emission	Annealed film[b]
1	439	447	448
2	438	446	455
3	439	451	456

[a]As 10^{-7} M THF. [b]As 250 nm thick films of polymer spun from toluene onto glass and measured as prepared (pristine) or heated (annealed) to 160 or 250 °C. Excitation at 365 nm.

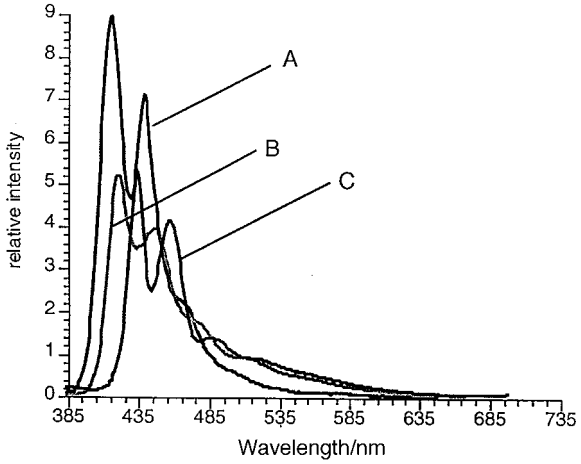

Fig. 3 Fluorescence spectra of **2**: A) as a 10^{-6} M solution in THF, O.D. = 0.1 at λ_{exc} = 355 nm under atmospheric conditions; B) as a 250 nm pristine (amorphous) film; and C) film (B) annealed to 160 °C.

shows the red-shifted emission observed upon going from solution to a pristine film to an annealed film of **2**.

In going from solution to the thin film, **1–3** show a significant red-shifted emission, with **3** exhibiting the greatest shift (Table 3). This suggests that the longer alkyl chains enhance interchain interactions, which leads to a more planar extended excited state for **3**. Annealing films of **2** and **3** causes a further red-shift, but no further shift in the annealed films of **1**, which suggests that interchain interactions induce a red-shift from the maxima observed in pristine films of **2** and **3**.

Fig. 4 shows the effect of annealing on the spectrum of a pristine film of **1** where no further red-shifts are observed in going from pristine-to-annealed films, but where increased fluorescence efficiency is observed at longer wavelengths. The absence of further red-shifts in **1** from pristine-to-annealed

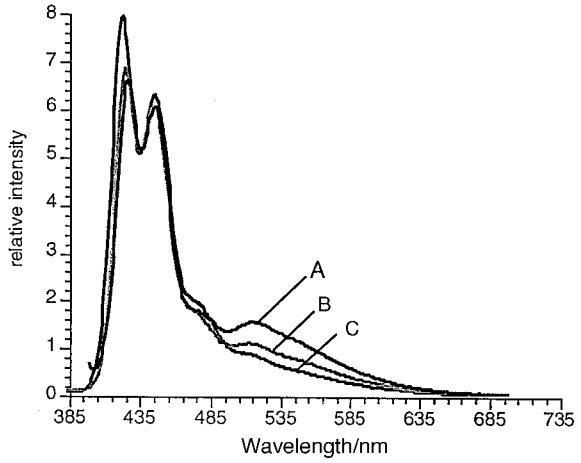

Fig. 4 Fluorescence spectra of 250 nm film of **1** with an O.D. = 0.5 at λ_{exc} = 355 nm under atmospheric conditions: A) as a pristine (amorphous) film; B) film annealed to 180 °C; and C) annealed to 250 °C. Fluorescence intensities of spectra are normalized at 440 nm.

films suggests that planarization is already sufficient to achieve maximum effective conjugation length beyond which annealing has no further effect.

The increased fluorescence efficiency observed at lower energies in films of **1–3** has been assigned to both aggregate and excimer emission, an assignment made in corroboration of assertions of Grell *et al.*[8] and Bliznyuk.[13] In going from solution to a pristine film to the annealed film, enhancement of the low energy transition is greater in **1** than in **3** or **2**. This observation implies that greater insulation of the polymer backbone by alkyl chains longer than six carbons does not affect the formation of excimer. Similarly, the larger red-shifts and lower energy of emission observed in films than in solution and in annealed films than in pristine films suggest that the polymer's ability to adopt a more planar excited state in films is facilitated by greater interchain interaction.

The variation in the red-shifted emission observed in going from homogeneous solution to a pristine film to an annealed film of **1–3** suggests that alkyl chain length significantly alters the supramolecular packing and thus the energy of emission (greater effective conjugation as a result of the extended rigid conformation and/or more favorable excimer formation). The mechanism of excimer formation is unclear. Longer alkyl chains induce greater order in pristine films, as evidenced by the greatest red-shift and the largest fractional contribution of the long-lived emitting species in **3**.

3.3. Fluorescence lifetimes

Fluorescence decays collected at 440 nm for **1–3** in THF were fitted to a single exponential to give approximately 550 ps lifetimes, Table 4. These lifetimes are independent of excitation and collection wavelength. Given an absence of any intermolecular interactions in dilute solutions of **1–3** in THF, the emissive species is assigned as an S_1,S_0 singlet exciton. When the same measurement is made in *n*-heptane (to induce aggregation), a transient emitting at 440 nm exhibited a lifetime of 430 ps (93%) with a small contribution from a new 700 ps species. Two longer lived species, 2 ns (7%) and 8 ns (4%), were also observed at 550 nm that were not present in solutions of similar concentration in THF (Table 4). These new longer lived transients at 550 nm are assigned to excimer and aggregate emission respectively,[27] and similar lifetimes were also observed in annealed films of **1–3** in the same spectral region, Table 5.

In films of **1–3**, the lifetime of the singlet exciton is reduced to between 200 and 300 ps at 440 nm because of an increase in possible non-radiative decay pathways. These include energy transfer to aggregate and excimer states and access to a greater number of contacts with the chain ends where exciton quenching is thought to be more efficient.[35] At 550 nm, fluorescence decays of pristine films of **1** and **3**, respectively, gave three single exponential lifetimes, respectively: 300 and 400 ps, 1 and 3 ns, and 10 and 12 ns, whereas films of **2** gave only two single exponential lifetimes of approximately 700 ps and 9 ns. Upon annealing past the second nematic phase of **1–3**, a decrease in the fluorescence intensity from the picosecond-lived species is observed, with a greater fraction of the fluorescence emanating from the longer-lived nanosecond species (Table 5). These lifetimes and fractional contributions were not constant over wavelength in the measured range of 500–600 nm. At present, it is not possible to unambiguously assign the 1–3 and 10–12 ns species at 550 nm in **1–3**, but they are thought to result from excimer and aggregate, respectively. Decays were collected at both 300 and 340 nm excitation for pristine and annealed films of **1–3** with similar results.

Because **2** forms aggregate most readily in solution and because this aggregation process is enhanced in films, aggregate formation likely dominates the interchain interactions, at the expense of excimer formation. Thus, the absence of the 1–3 ns

Table 4 Poly(dialkylfluorene) solution fluorescence lifetimes and fluorescence quantum yields

Polymer	τ_{fl}/ns (% composition), ± 0.03 ns	$\lambda_{emission}$/nm	χ^2	$\Phi_{fl}{}^b \pm 0.01$
1[a]	0.56 (100)	440	1.09	0.64
2[a]	0.52 (100)	440	1.07	0.69
2[c]	0.43 (93), 0.72 (7)	440	1.49	0.51
2[c]	0.51 (89), 1.93 (7), 8.35 (4)	550	1.06	
3[a]	0.55 (100)	440	1.19	0.65

[a]Lifetimes determined with excitation at 300 nm in 10^{-7} M THF. [b]Quantum yields (Φ_{fl}) determined in cyclohexane relative to 9,10-diphenylanthracene with excitation at 365 nm.[33] [c]Lifetimes determined in 10^{-7} M *n*-heptane to induce aggregation.

Table 5 Poly(dialkylfluorene) film fluorescence lifetimes[a] and quantum yields[b]

	Annealing temp./°C	$\tau_{fl}/\pm 0.03$ ns (% contribution) $\lambda_{obs}=440$ nm	χ^2	$\tau_{fl}/\pm 0.3$ ns (% contribution) $\lambda_{obs}=550$ nm	χ^2	$\Phi_{fl} \pm 0.1$ (%)
1	25	0.27 (100)	5.64	0.3 (94), 1.3 (5), 10.2 (1)	32.86	15.5
	250	0.18 (100)	87.9	0.2 (54), 3.0 (19), 11.8 (27)	2.83	10.0
2	25	0.29 (100)	4.56	0.7 (91), 9.1 (9)	3.68	17.0
	160	0.21 (100)	1.70	0.7 (86), 9.8 (14)	11.5	25.5
3	25	0.32 (93), 0.77 (7)	1.14	0.4 (88), 3.2 (6), 12.3 (6)	1.40	15.5
	160	0.31 (96), 0.81 (4)	1.09	0.4 (77), 3.2 (7), 11.6 (16)	1.99	13.5

Measurements with 250 nm films on glass. [a]Lifetimes (τ_{fl}) measured using single photon counting[23] with $\lambda_{exc}=340$ nm with 250 nm films. [b]Quantum yields (Φ_{fl}) measured using integrating sphere technique[25] where each value is an average of 2–3 measurements with approx. 10% relative standard deviation.

species in **2** (rather than in **1** and **3**) suggests that the 9–12 ns species in **1–3** can be assigned to aggregates and that **2** already has an optimal configuration that inhibits excimer formation. In films of **1** and **3** where both aggregate and excimer are present, the total contributions from both of the two long-lived (ns) species are 46% in **1** and 23% in **3**. Thus, shorter alkyl chains likely permit better supramolecular packing of **1**, which in turn produces greater interchain communication. The long lived species observed in films of **1–3** and the increased fractional contribution of these species as the films are annealed are evidence of enhanced interchain interactions resulting from the nematic ordering of the alkylated polymer chains.

3.4. Fluorescence quantum yields

The dependence of fluorescence quantum yields on supramolecular packing was probed by measuring the changes in fluorescence quantum yields observed upon moving from solution to film and upon increasing local ordering of the thin films through annealing. The fluorescence quantum yields of **1–3** in cyclohexane ranged between 51 and 69%, dependent on polymer concentration, Table 4. Thus, aggregation induces a lowering of the quantum yield by approximately 20%.

Pristine films of **1–3** have identical quantum yields of approximately 16%, Table 5.[36,37] This dramatic decrease from the observed solution quantum yields suggests that stronger interactions between chains in the films drastically lowers fluorescence quantum yields. This is similar to the value reported by Redecker *et al.*[12] (0.50) for the fluorescence quantum yield, where the value was quite dependent on film morphology. Upon annealing (past their second nematic phase) to induce greater order, films of **3** show no change in the observed fluorescence quantum yield, whereas films of **2** show a slight increase. When films of **1** were annealed past their second nematic phase transition temperature, the quantum yields decreased slightly from 15.5 to 10%. The phase transition temperatures vary between **1–3**, so it was possible that changes in quantum yield might be due to temperature dependent fluorescence impurity quenching rather than to supramolecular packing induced by liquid crystalline phase transition. However, control experiments in which **2** and **3** are annealed at the same transition temperature as **1** showed the same results. Thus, the decrease in quantum yield of **1**, but not of **2** or **3**, suggests that shorter alkyl chains allow for better interpolymer interaction, thus reducing the observed fluorescence efficiency. The unexpected increase in fluorescence quantum yield for annealed films of **2** suggests that the **1–3** ns-lived species present in **1** and **3** (but not in **2**) may be responsible for the efficient fluorescence quenching. Thus, an optimal alkyl chain length produces the highest fluorescence efficiency in these alkyl-substituted polyfluorene films.

4. Conclusions

The degree of interpolymer interactions in 9,9-dialkylated polyfluorenes in solution can be controlled by choice of solvent and by the length of the alkyl chain. The degree of interchain interaction in solution is greatest for **2**, followed by **1** and **3**, as evidenced by the relative intensities of a new 437 nm aggregate band, even in good solvents. Pristine films of **3** show greater red-shifts in emission bands from solution maxima than do those of **1** or **2**. Annealing produces further red-shifts in **2** and **3**, but not in **1**. Thus, longer alkyl chains force an extended ground state conformation, the planarity of which in turn enhances intermolecular aggregation in solution. Polyfluorenes bearing longer alkyl chains will thus exhibit enhanced on-axis dipole moments and increased dichroic ratios.

Films of **1**–**3** show increased ordering upon annealing, as evidenced by formation of an oriented nematic liquid crystalline phase that shows a characteristic Schlieren texture. Although the exact identity of the ns-lived species cannot be exactly determined with this data, the contribution of this species is greatest in **1**, implying that greater excited state interchain communication is possible with the polyfluorenes bearing the shorter alkyl chains. This packing, in turn, leads to enhanced excimer formation. The fluorescence quantum yields in these polymers decrease from 51–69% in solution to approximately 3% as pristine films, implying substantial fluorescence quenching in the as-deposited thin films of **1–3** as a function of packing. The fluorescence quantum yield of **1** decreases slightly upon annealing, whereas those of **2** and **3** increase and remain the same, respectively. This suggests that the shorter alkyl chains enhance interchain packing interactions, with predictable consequences for fluorescence efficiency in these films.

Acknowledgements

We gratefully acknowledge Drs Edward P. Woo and Michael Inbaskeran at Dow Chemical for samples of polyfluorenes **1–3** and for useful discussions of this work. We acknowledge Donald O'Connor of the Center for Fast Kinetics at the University of Texas at Austin for assistance with the time-resolved fluorescence measurements. This work was supported by the Texas Advanced Research Program and the Robert A. Welch Foundation.

References

1 J. H. Burroughes, R. H. Friend, D. D. C. Bradley, A. R. Brown, R. N. Marks, K. Mackay, P. L. Burn and A. B. Holmes, *Nature*, 1990, **347**, 539.
2 A. Heeger, F. Hide, B. Schwartz and M. A. Diaz-Garcia, *Chem. Phys. Lett.*, 1996, **256**, 424.
3 H. Sirringhaus, N. Tessler and R. H. Friend, *Science*, 1998, **280**, 1741.
4 C. Weder, C. Sarwa, A. Montali, C. Bastiaansen and P. Smith, *Science*, 1998, **279**, 835.
5 M. Fukuda, K. Sawada and K. Yoshino, *Jpn. J. Appl. Phys.*, 1989, **28**, L1433.
6 M. Fukuda, K. Sawda and K. Yoshino, *J. Polym. Sci., Part A: Polym. Chem.*, 1993, **31**, 2465.
7 M. Grell, D. D. C. Bradley, M. Inbasekaran and E. F. Woo, *Adv. Mater.*, 1997, **9**, 798.
8 D. D. C. Bradley, M. Grell, X. Long, H. Mellor and A. Grice, *Soc. Phot. Int. Eng.*, 1997, **3145**, 254.
9 Q. Pei and Y. Yang, *J. Am. Chem. Soc.*, 1996, **118**, 7416.
10 Y. Ohmori, M. Uchida, K. Muro and K. Yoshino, *Jpn. J. Appl. Phys., Part 2*, 1991, **30**, L1941.
11 M. Grell, D. D. C. Bradley, X. Long, T. Chamberlain, M. Inbasekaran, E. P. Woo and M. Soliman, *Acta Polym.*, 1998, **49**, 439.
12 M. Redecker, D. D. C. Bradley, M. Inbasekaran and E. P. Woo, *Appl. Phys. Lett.*, 1998, **73**, 1565.
13 V. N. Bliznyuk, S. A. Carter, J. C. Scott, G. Klarmer, R. D. Miller and D. C. Miller, *Macromolecules*, 1999, **32**, 361.
14 C. E. Halkyard, M. E. Rampey, L. Kloppenburg, S. L. Studer-Martinez and H. F. Bunz, *Macromolecules*, 1998, **31**, 8655.
15 G. Grem, B. Keditzky, D. Ullrich and G. Leising, *Adv. Mater.*, 1992, **4**, 36.
16 S. Tasch, A. Niko, G. Leising and U. Scherf, *Appl. Phys. Lett.*, 1996, **68**, 1090.
17 Y. Yang, Q. Pei and A. J. Heeger, *J. Appl. Phys.*, 1996, **79**, 934.
18 A. W. Grice, A. Tajbakhsh, P. L. Burn and D. Bradley, *Adv. Mater.*, 1997, **9**, 1174.
19 (*a*) G. Wegner, D. Neher, M. Remmer, V. Cimrova and M. Schulze, *Mater. Res. Soc. Symp. Proc.*, 1996, **413**, 23; A. Kraft, A. C. Grimsdale and A. B. Holmes, *Angew. Chem., Int. Ed.*, 1998, **37**, 402.
20 C. Weder, J. M. Wagner and M. S. Wrighton, *Mater. Res. Soc. Symp. Proc.*, 1996, **413**, 77.
21 C. Weder and M. S. Wrighton, *Macromolecules*, 1996, **29**, 5157.
22 J. W. Blatchford, S. W. Jessen, L. B. Lin, T. L. Gustafson, D. K. Fu, H. L. Wang, T. M. Swager, A. G. MacDiarmid and A. J. Epstein, *Phys. Rev. B*, 1996, **54**, 9180.
23 U. Lemmer, S. Heun, R. F. Mahrt, U. Scherf, M. Hopmeier, U. Siegner, E. O. Gobel, K. Müllen and H. Bässler, *Chem. Phys. Lett.*, 1995, **240**, 373.
24 S. A. Jenekhe and J. A. Osaheni, *Science*, 1994, **265**, 765.
25 T. Pauck, R. Hennig, M. Perner, U. Lemmer, U. Siegner, R. F. Mahrt, U. Scherf, K. Müllen, H. Bässler and E. O. Gobel, *Chem. Phys. Lett.*, 1995, **244**, 171.
26 I. D. W. Samuel, G. Rumbles, C. J. Collison, B. Crystall, S. C. Moratti and A. B. Holmes, *Synth. Met.*, 1996, **76**, 15.
27 E. Conwell, *Trends Polym. Sci.*, 1997, **5**, 218.
28 D. V. O'Conner and D. Phillips, *Time-Correlated Single Photon Counting*, Academic Press, London, 1984.
29 D. Eaton, *Pure Appl. Chem.*, 1988, **60**, 1107.
30 J. C. de Mello, F. H. Wittmann and R. H. Friend, *Adv. Mater.*, 1997, **9**, 230.
31 M. Balauff, *Macromolecules*, 1986, **19**, 1366.
32 L. C. Sawyer and D. T. Grubb, *Polymer Microscopy*, Chapman & Hall, London, 1996.
33 N. H. Hartshorne, *Optical Properties of Liquid Crystals: Physico-Chemical Properties and Methods of Investigation*, Horwood, Chichester, 1974, Vol. 2.
34 B. A. Wood and E. L. Thomas, *Nature*, 1986, **324**, 655.
35 C. Weder and M. S. Wrighton, *Macromolecules*, 1995, **29**, 5157.
36 In measuring quantum yields for thin films, variations in refractive index, surface roughness, and film thickness can introduce inconsistency into the measurement of fluorescence quantum yields.[31] Therefore, an integrating sphere was employed to measure the quantum yields for the thin films.
37 N. C. Greenham, I. D. W. Samuel, G. R. Hayes, R. T. Phillips, Y. A. R. R. Kessener, S. C. Morratti, A. B. Holmes, R. H. Friend, *Chem. Phys. Lett.*, 1995, **241**, 89.

Paper 9/02829C